Proceedings of the 2019 Design of Medical Devices Conference
DMD2019
April 15, 16-18, 2019, Minneapolis, MN, USA

DMD2019-3315

TOWARDS A GENERALIZED MODEL OF MULTIVARIABLE ANKLE IMPEDANCE DURING STANDING BASED ON THE LOWER EXTREMITY MUSCLE EMG

Lauren N. Knop, Guilherme A. Ribeiro,
Michigan Technological University
Department of Mechanical Engineering – Engineering Mechanics
Houghton, MI, USA

Mo Rastgaar[1]
Purdue University
Polytechnic Institute
West Lafayette, IN, USA

ABSTRACT

The ankle mechanical impedance of healthy subjects was estimated during the standing pose while they co-contracted their lower-leg muscles. Subsequently, the impedance parameters were modeled as a function of the level of co-contraction using machine learning regression methods. From the experimental results, the average ankle stiffness coefficients in dorsi-plantar flexion (DP) showed more dependence to the muscle contraction than stiffness in inversion-eversion (IE): 4.6 Nm/rad per %MVC (percent of the maximum voluntary contraction) and 1.1 Nm/rad per %MVC, respectively. To accurately estimate the ankle impedance parameters as a function of the electromyography (EMG) signals, multiple EMG feature selection methods, regression models, and types of models were evaluated. Using a 1-vs-All model validation approach, the best regression model to fit the stiffness and damping in DP was the Least Square method with Regularization, and the best IE stiffness was the Gaussian Process Regression. No model was able to estimate the IE damping well, possibly because this parameter is not modulated with a changing co-contraction of the lower-leg muscles.

Keywords: ankle impedance, electromyography, regression, machine learning, non-linear optimization

1. INTRODUCTION

As the development in areas such as active prostheses, exoskeletons, and neuromuscular rehabilitation continues to expand, so has the need to better understand how the end user interacts with the device. Previous literature suggests that surface electromyography (EMG) could be an essential element in predicting a user's motion intention, especially with the wide variety of machine learning techniques that are available [1-4].

One approach studies the continuous relationship between muscle activation and joint motion. In [5], proportional control was also used to actively control the dorsi-plantar flexion (DP) motion using an amputee's residual EMG signals. A nonlinear autoregressive model predicted the DP ankle angle for an ankle-foot prosthesis during walking using the amputee's residual EMG signals within the socket [6]. In [7], the relationship between muscle contraction level and healthy ankle impedance was studied in both the DP and inversion-eversion (IE) directions. As expected, ankle stiffness generally increased with higher muscle activation; however, not all subjects exhibited a linear relationship. To better explain this relationship, an Artificial Neural Network (ANN) with a single hidden layer was implemented [8, 9]. The resulting subject-dependent models were able to predict ankle impedance in DP and IE directions with greater than 95% accuracy using the corresponding lower extremity muscle co-contraction levels. However, these models were subject dependent and did not perform well with input EMG signals from a different subject.

In parallel to these EMG studies, previous work determined the ankle mechanical impedance in the dorsi-plantarflexion (DP) and inversion-eversion (IE) directions under loaded and non-loaded scenarios [10-14]. The mechanical impedance of the ankle is defined as the ankle's response to an input motion and can be useful in the control design of active ankle-foot prostheses [12]. Commonly, the ankle impedance is modeled as a second order system and is described in terms of stiffness, damping, and inertial properties of the ankle and foot.

The purpose of this study was to examine ways to improve the performance of a generalized model that can estimate ankle impedance based on a subject's EMG signals that were unseen to the model during training. Previous work by the authors studied the relationship between standing ankle impedance and lower extremity muscle co-contraction level [8, 9]. These studies determined the performance of (1) an individual ANN model optimized for each separate subject, (2) an aggregated ANN model, which used the data of all the subject population (12 subjects) to train and test a single ANN model, and (3) a "1-vs-All" method, where a model was trained with the data of $N-1$ subjects and the performance was tested with the remaining subject to verify the generalization of the model. When comparing the three methods, the individual models had the highest performance (average R^2 >0.86), followed by the aggregate model (average R^2 >0.82). While these models had a

[1] Contact Author: rastgaar@purdue.edu
*Research supported by NSF grants 1350154 and 1830460.

reasonable performance, they were not able to predict the impedance of an unseen subject not used to train the model. The "1-vs-All" method determined an average R^2 of 0.65 for K_{DP} and less than 0.2 for K_{IE}, B_{IE}, and B_{DP}.; showing that the generalized method was much lower than methods (1) and (2). The goal of this study was to increase the model accuracy by improving the stiffness and damping parameters estimation of the 2- degree of freedom (DOF) ankle impedance, increasing the number of features that were extracted from the EMG signals, and testing these features on a wider variety of regression models. When compared to previous work, this study showed feasible steps towards improving the performance of a generalized model.

2. METHODS

2.1 Subjects

All participants gave written informed consent to participate in this study, which was approved by the Michigan Technological University Institutional Review Board. Eleven healthy male subjects were recruited with an average age of 28 ± 3.7 years, average weight of 93.3 ± 28.8 kg, an average height of 180 ± 6.9 cm and no previous history of biomechanical or neuromuscular disorders.

2.2 Experimental Procedure

The same experimental procedure was used in our previous studies [8, 9], which estimated standing ankle impedance with the use of the instrumented platform. This platform (Fig. 1) consisted of a vibrating platform, force plate (Kistler 9260AA3), and a motion capture system (8 x Optitrack 17W). The standing ankle impedance was determined by exciting the ankle in both the DP and IE directions with a stochastic perturbation (up to 33 Hz), and measuring the resultant ground reaction forces, ground reaction torques, and ankle rotations. Wireless surface EMG sensors (Delsys® Trigno™ Wireless System) were placed on the tibialis anterior (TA), peroneus longus (PL), soleus (SOL), and gastrocnemius (GA) muscles to measure muscle contractions. These muscles were selected based on their contribution to ankle stabilization and rotation [15].

The experiment included a total of 10 trials where stochastic perturbations were applied to the subject's right foot for approximately 70 seconds. During each trial, the subject stood with their muscles co-contracted at a selected level, including no co-contraction, and actively co-contracting to 10%, 20%, 30%, or 40% maximum voluntary contraction (MVC). Each muscle activation level was performed in a randomly selected order and was repeated once while their foot was placed at 0 degrees and again with their foot at 90 degrees, with respect to the force plate coordinate frame (Fig. 1). The purpose of rotating the foot locations was to better separate the inertia of the force plate and foot bodies during the impedance estimation.

The subject's MVC was determined at the beginning of the experiment by co-contracting their muscles to their maximum level for approximately a 1-second interval. This process was repeated 5 to 10 times, and the highest maximum voltage of the TA muscle was selected to be the reference MVC for the remainder of the trials. During the 10 trials, the subject received visual feedback of their real-time muscle contraction and the target voltages, determined as a percentage of the MVC. Subjects

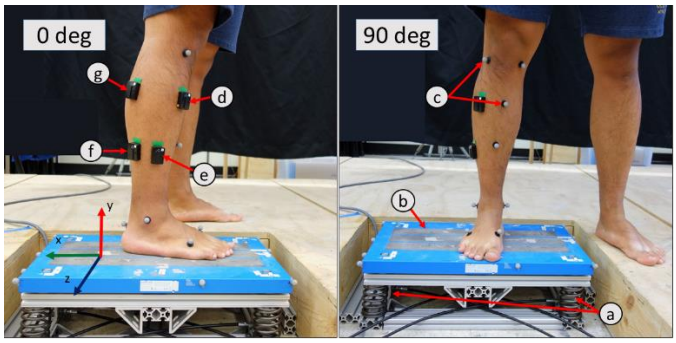

Figure 1. *Experimental setup while subject was standing at 0 degrees and 90 degrees with respect to the force plate coordinate. Setup included (a) the vibrating platform, (b) force plate, (c) motion capture reflective markers, (d – g) TA, PL, SOL, and GA EMG muscle sensors.*

maintained the voltage level of their muscle as best as they could to match the target line for the duration of the 70-second trial. In between trials, subjects rested for a few minutes to reduce the effects of fatigue.

2.3 Data Acquisition

The motion capture system and the force plate module were both sampled at 350 Hz to capture the kinematic and kinetic data. The EMG was measured with a sampling rate of 2000 Hz and was low passed filtered at 500 Hz. In addition, the Delsys® software included a motion artifact suppression to reduce the effects of low-frequency noise.

3. STANDING ANKLE IMPEDANCE ESTIMATION

The multivariable mechanical impedance of the ankle was estimated using the differential equations of motion of the lower leg that included the ankle impedance coefficients and the inertia of the foot and force plate. This method approximates the foot as a rigid body and the ankle as a gimbal joint with a spring and viscous damper on each rotating axis.

The differential equation is derived from the conservation of angular momentum, resulting in

$$\begin{aligned} &I_P\dot{\omega}_P + \omega_P \times (I_P\omega_P) + R_P^T\{(p_{P0} - p_F) \times \\ &[m_P(\ddot{p}_{P0} - g)] \ + R_F[I_F\dot{\omega}_F + \omega_F \times (I_F\omega_F)] + \\ &(p_{F0} - p_F) \times [m_F(\ddot{p}_{F0} - g)] + R_F T_Z(\theta, \dot{\theta})\} \\ &= T_P + T_{bias} + R_P^T[(p_P - p_F) \times (F_P + F_{bias})] \end{aligned} \quad (1)$$

where $I_i = \begin{bmatrix} Ixx_i & Ixy_i & Ixz_i \\ Ixy_i & Iyy_i & Iyz_i \\ Ixz_i & Iyz_i & Izz_i \end{bmatrix} \in \mathbb{R}^{3\times3}$, $\dot{\omega}_i \in \mathbb{R}^3$, $\omega_i \in \mathbb{R}^3$, $R_i \in SO(3)$, $p_{i0} \in \mathbb{R}^3$, $p_i \in \mathbb{R}^3$ and $m_i \in \mathbb{R}^+$ are the inertial tensor on the body frame, local angular acceleration, local angular velocity, rotation matrix, global position of the center of mass and coordinate frame, and mass of body i, respectively, for either body P (force plate) or F (foot). In addition, $g \in \mathbb{R}^3, T_P \in \mathbb{R}^3, F_P \in \mathbb{R}^3, T_{bias} \in \mathbb{R}^3$ and $F_{bias} \in \mathbb{R}^3$ are the gravity vector, torque and force measured by the force plate at its origin, and torque and force sensor biases. The internal torque resulted from the ankle spring and damper are

$$T_Z(\theta, \dot{\theta}) = \frac{1}{c\theta_2}\begin{bmatrix} c\theta_3 & -s\theta_3 & 0 \\ c\theta_2 s\theta_3 & c\theta_2 c\theta_3 & 0 \\ -s\theta_2 c\theta_3 & s\theta_2 s\theta_3 & c\theta_2 \end{bmatrix}\left(K^{diag} + B^{diag}\dot{\theta}\right) \quad (2)$$

where $\theta \in SO(3)$, $K^{diag} \in \mathbb{R}^3$, and $B^{diag} \in \mathbb{R}^3$, are the joint angles, and diagonal matrices of stiffness and damping, for a Euler rotation order of XYZ from shin to foot frame. The matrix composed with θ converts the torques from the Euler axis to the foot frame. Finally, the kinematic variables that depend on the unknown parameters are calculated as

$$\begin{cases} p_{P0} = p_P + R_P r_P & (3.a) \\ p_{F0} = p_F + R_F r_F & (3.b) \end{cases}$$

$$\begin{cases} \ddot{p}_{P0} = \ddot{p}_P + R_P[\dot{\omega}_P \times r_P + \omega_P \times (\omega_P \times r_P)] & (4.a) \\ \ddot{p}_{F0} = \ddot{p}_F + R_F[\dot{\omega}_F \times r_F + \omega_F \times (\omega_F \times r_F)] & (4.b) \end{cases}$$

where $\ddot{p}_i \in \mathbb{R}^3$ and $r_i \in \mathbb{R}^3$ are the linear acceleration of any body i.

The derivatives from equations (1-4) were calculated with a Sarvitzky-Golay filter [16] with 11-samples window and a 5th order polynomial. In addition, the same filter was used to smooth all the other kinematic signals. This filter approximates the samples of a signal within a moving window as a polynomial and calculates derivatives with good noise rejection.

The best estimates for the unknown parameters were calculated with the non-linear optimization method, Sequential Quadratic Programming [17], substituting the measurements and computed derivatives into Eq. 1, and reducing the mean-square-error of the equation. To improve the stability of the results, the force plate inertia parameters were estimated in a separate experiment, in which the platform vibrated without any human load. In addition, to account for sensor biases and time-varying impedance, different values of T_{bias}, F_{bias}, K and B were estimated in small sample windows. Therefore, the vector of unknown parameters is

$$x \equiv [J_F, m_F, r_F, z^{[1]}, z^{[2]}, \dots, z^{[10]}] \quad (5)$$

$$z^{[t]} \equiv [T_{bias}^{[t]}, F_{bias}^{[t]}, K^{[t]}, B^{[t]}] \quad (6)$$

where $z^{[t]}$ is the set of biases and impedances of trial t. Considering the impedance and bias might change even within a trial, each trial was split in 40 sections (with overlap) of 2-seconds of duration and used to estimate an independent solution, x. Therefore, each subject had 40 estimates of foot inertia, and 400 estimates of ankle impedance.

4. FEATURE EXTRACTION

To avoid under or overfitting of a model during training, the input feature vector should describe the useful characteristics found in the raw data. In addition, the number of features selected also plays a factor in how well the model can be trained. Too few features might cause a model to be underfitted and too many features may cause linearly dependent features to overfit to a model. This paper looked at the effects of feature selection on model performance.

4.1 EMG Signal

Figure 2 shows the averaged and z-score normalized EMG signals across the entire population, while the subject co-contracted their muscle from 0% to 40% of their MVC. The general trend shows that the EMG voltage increased linearly with muscle activity, with the exception of the SOL muscle.

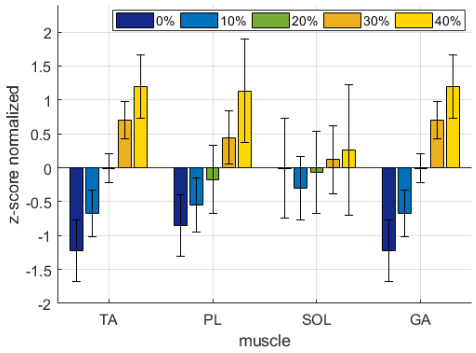

Figure 2. Average ± standard deviation of the z-score normalized EMG signals for the TA, PL, SOL, and GA muscles across the 5 co-contraction levels.

Information from each of the EMG signals was concatenated into a single input feature vector and used to train each regression fitting model.

4.2 Time Domain Features

Six simple time domain (TD) features were selected for this study, including: the mean (AVE), standard deviation (STD), mean absolute value (MAV), number of zero crossings (ZC), number of slope sign changes (SSC), and the cumulative length of the signal (CL). These features were selected based on previous work and are described in [2, 18-21]. The features provide insight towards the amplitude, frequency, and scale of the signal. Each feature extraction method was applied to the windows of all four EMG channels in each trial.

4.3 Normalization

All data were normalized using z-score normalization. This method was selected to resize the EMG and impedance parameters to a similar scale, which can greatly improve training and testing results. This normalization is shown as

$$\bar{x} = \frac{x_i - \mu_x}{\sigma_x} \quad (7)$$

where x is the sample being normalize, μ is the mean, and σ is the standard deviation across the population of interest.

After the data was separated into windows, outliers from the EMG and impedance parameters were removed, and the parameters were z-score normalized by individual subjects. This reduced any large differences in amplitudes between impedance and EMG. Additionally, the impedance parameters were normalized by the subject's weight. After the EMG features were extracted, the EMG and impedance parameters were once more z-score normalized, this time across the entire population.

5. REGRESSION MODEL SELECTION

Several commonly used regression models have been proposed to estimate ankle impedance using EMG signals [4, 22]. The goal was to determine a model or a group of models that can estimate this relationship with high performance. Using the MATLAB Regression Learner App, *fitrlinear* function, and the Neural Network Fitting App, the following regression models were selected for this study, including:

1. Least Squares Linear Regression (*LSQ*)
2. Least Squares linear regression with Lasso Regularization (*LSQ + Reg*)
3. Medium Gaussian Support Vector Machine (*SVM*)

4. Support Vector Machine with Lasso Regularization (*SVM + Reg*)
5. Gaussian Process Regression with Matern 5/8 Kernel (*GPR*)
6. Single Layer Artificial Neural Network (*ANN*)

5.1 Training & Testing

Each model was trained using the training data set, which consisted of EMG features (ranging from 4 up to 24) as inputs and 4 impedance parameters as the target. Three methods of training were tested, as previously described in [8]. The first method included generating an individual model for each of the subjects and testing the performance using only the data from the subject-specific model. While this method is not a generalized solution, it has shown to have the highest performance and was used to test the effects of EMG features selection on model performance.

Using the best-performing feature vector from the individual model study, the regression models were tested using an aggregated model and trained using the data from the total population (11 subjects). In addition, these regression models were tested to estimate impedance when given unseen EMG data using the 1-vs-All technique. This technique trained each model using 10 out of 11 subjects, and then tested the model's performance with the 11th subject. The model iterated so that all the subjects were used during testing.

5.2 Performance Evaluation

The performance of each regression model was determined by comparing the predicted impedance parameters, $\hat{Z}$, with the nominal impedance parameters, Z, used during training. The measure of how well the predicted compared to the actual impedance was determined using the normalized mean-squared-error, as described in Eq. 8, where μ_z is the mean of the nominal impedance.

$$NMSE = 1 - \frac{\|\hat{Z} - Z\|^2}{\|\hat{Z} - \mu_Z\|^2} \quad (8)$$

Before calculating the NMSE, both the predicted and nominal impedance parameters were first de-normalized or converted back into their original units. By re-scaling the impedance, there is a better understanding of the relative error. For the three types of models (individual, aggregated, and 1-vs-All), the NMSE was determined using the *'goodnessoffit'* function in MATLAB and the predicted and nominal impedance vectors of all the subjects, where $\hat{Z} = \{\hat{z_1}, \hat{z_2}, \dots \hat{z_{11}}\}$ and $Z = \{z_1, z_2, \dots, z_{11}\}$.

6. RESULTS

6.1 Impedance Identification

The unknown parameters resulted in a mean torque error of the reconstructed torque of 2.1 ± 0.3 Nm amongst all solutions. The mean torque error describes the error between the nominal and estimated torque vectors and is defined as

$$\varepsilon(\boldsymbol{x}) = \frac{1}{N}\sum_{i=1}^{N}\left\|\boldsymbol{T}_{est}^{[i]}(\boldsymbol{x}) - \boldsymbol{T}_{ref}^{[i]}\right\|_2 \quad (9)$$

where $\boldsymbol{T}_{est}^{[i]}(\boldsymbol{x})$ and $\boldsymbol{T}_{ref}^{[i]}$ are the estimated and reference ground reaction torque around the ankle (isolating $T_P + R_P^T[(p_P - p_F) \times F_P]$ from Eqn. 9), for the i^{th} of N samples.

According to the resulting estimated ankle impedance, both the ankle joint stiffness and damping have shown dependence to the co-contraction on the lower-leg muscles. The curve of Fig. 3 was approximated to a linear equation, resulting in an average impedance during the passive trial (curve intercept) and the change of impedance per unit of muscle co-contraction (curve slope). The R^2 for the linear equations were 0.74, 0.97, 0.09, and 0.96 for KIE, KDP, BIE, and BDP, respectively.

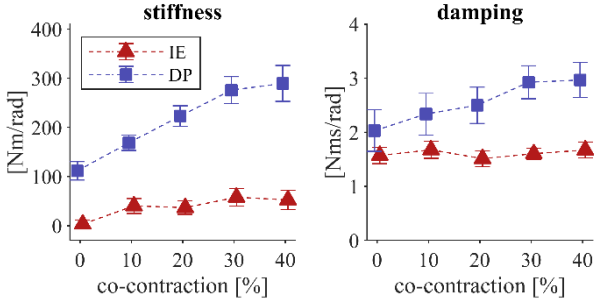

Figure 3. Resulting average ± MAE of the impedance across eleven subjects in both the DP and IE directions. The MAE is amongst the means of each subject in the respective trial.

In response to a co-contraction increase, the ankle stiffness increased four times more in the DP than in IE anatomical axis. The IE damping showed a low linear fitness score (R^2 = 0.09), suggesting a weak linear correlation. Similar characteristics of ankle stiffness and damping have been determined at varied muscle contraction levels while the ankle was non-loaded [7, 23]. The stiffness in DP was greater than the stiffness in IE for all contraction levels and the damping parameter typically had a smaller change over contraction levels, consistent with results found in [7].

TABLE 1: LINEAR FIT BETWEEN MUSCLE CO-CONTRACTION AND ANKLE IMPEDANCE

	K_{IE}	K_{DP}	B_{IE}	B_{DP}
	Nm/rad		Nms/rad	
Passive Impedance (Intercept)	14.7	121.1	1.6	2.1
Impedance change (per % MVC)	1.1	4.6	1.3×10^{-3}	24.6×10^{-3}

6.2 Regression Model Training

Feature Extraction. The results in Table 2 show the NMSE for 6 regression model types and 4 different combinations of TD EMG features. All models were trained using individual models and the NMSE was determined using Eq. 8. As the number of features selected increased, the model fitness was improved. When comparing the four combinations of feature vectors, the vector that contained all 24 features

TABLE 2: TD FEATURE EXTRACTION EFFECT ON MODEL PERFORMANCE FOR INDIVIDUAL SUBJECT MODELS.

		LSQ	LSQ + Reg.	SVM	SVM + Reg.	GPR	ANN (30)
(4) - STD	KIE	0.704	0.707	0.820	0.695	0.932	0.785
	KDP	0.460	0.717	0.828	0.695	0.905	0.764
	BIE	0.318	0.335	0.650	0.300	0.877	**0.681**
	BDP	0.809	0.810	0.883	0.802	0.963	0.916
(8) - STD + MEAN	KIE	0.734	0.737	0.864	0.724	0.924	**0.779**
	KDP	0.512	0.743	0.863	0.727	0.910	0.496
	BIE	0.476	0.479	0.784	0.455	0.861	0.470
	BDP	0.823	0.824	0.922	0.813	0.951	0.894
(16) - MAV, ZC, SSC, + CL	KIE	0.781	0.781	0.883	0.764	0.974	0.729
	KDP	0.803	0.807	0.886	0.792	0.916	0.758
	BIE	0.556	0.552	0.806	0.519	0.954	0.511
	BDP	0.872	0.871	0.947	0.861	0.985	**0.919**
(24) - STD, MEAN, MAV, ZC, SSC, + CL	KIE	**0.821**	**0.808**	**0.890**	**0.779**	**0.976**	0.762
	KDP	**0.817**	**0.817**	**0.888**	**0.801**	**0.918**	**0.796**
	BIE	**0.635**	**0.602**	**0.825**	**0.543**	**0.956**	0.632
	BDP	**0.903**	**0.884**	**0.950**	**0.867**	**0.989**	0.914

*all table data is the NMSE (R^2) between the predicted and actual measurement of total population

(AVE, STD, MAV, ZC, SSC, and CL) achieved the highest result for all model types. The 24-feature vector was selected to be used during the aggregated and 1-vs-All model testing.

Aggregated Regression Models. The aggregated model of the total population showed the highest performance when trained with the GPR model. The resulting NMSE was greater than 0.95 for all the impedance parameters (Table 4). This was the highest training performance across all models trained during this analysis.

TABLE 4: NMSE (R^2) FOR AGGREGATED MODEL OF TOTAL POPULATION

	K_{IE}	K_{DP}	B_{IE}	B_{DP}
LSQ	0.638	0.677	0.261	0.727
LSQ + Reg	0.642	0.683	0.268	0.733
SVM	0.828	0.841	0.651	0.898
SVM + Reg	0.632	0.682	0.253	0.710
GPR	**0.989**	**0.953**	**0.973**	**0.998**
ANN	0.797	0.784	0.548	0.893

1-vs-All Regression Models. The 1-vs-All models used the data of an unseen subject to test the performance of the model. The resulting NMSE can be found in Table 5. The highest NMSE was found using the LSQ + Reg model for B_{DP} with a value of 0.65. In addition, this model showed to have the highest performance for K_{DP} and B_{IE} with values of 0.589 and 0.098, respectively. One possible reason that the simpler models had the highest performance is because the other models overfit to the training data. By having fewer weights within the model, the impedance parameters were better explained by the EMG features. This also suggests that the ANN model overfits to the training data, resulting in the worst NMSE out of all the model types. Interestingly, K_{IE} has a slightly higher score using the GPR model with a value of 0.558.

TABLE 5: NMSE (R^2) FOR 1-VS-ALL TEST FOR GENERALIZABILITY

	K_{IE}	K_{DP}	B_{IE}	B_{DP}
LSQ	0.526	0.574	0.076	0.637
LSQ + Reg	0.540	**0.589**	**0.098**	**0.650**
SVM	0.525	0.585	-0.09	0.648
SVM + Reg	0.530	0.567	0.067	0.622
GPR	**0.558**	0.582	-0.005	0.663
ANN	0.417	0.484	-0.227	0.592

Another observation is that IE damping had a very poor performance across all the model types, with the highest value being 0.098. The results in Table 3 show that the change in the IE damping across the 5 muscle activation levels was small. This small change suggests that either the parameter was not modulated enough to be related to the muscle signal, or the parameter was more susceptible to noise in the model.

When comparing to the previous study [8], the results of the 1-vs-All method improved with the addition of new EMG features and new model types. The previous work, which used only an ANN model to relate EMG and impedance, resulted in an average NMSE of 0.67 for K_{DP}, 0.18 for K_{IE}, 0.19 for B_{DP}, and -0.07 for B_{IE}. The improvements in the 1-vs-All method show promising results towards a generalized model that can predict ankle impedance based on lower extremity muscle activations. Future work will test additional feature extraction methods not presented in this paper, such as exploring the frequency domain. It will also look to improve normalization methods, impedance estimation techniques, and increase the number of subjects during training.

7. CONCLUSION

In this work, the ankle mechanical impedance of 11 healthy subjects was estimated during standing while they co-contracted their lower-leg muscles. Subsequently, the impedance

parameters were related to the level of co-contraction using regression and machine learning techniques.

The predicted impedance parameters were able to explain the effect of an external torque to the ankle motion with an error of 2.1 ± 0.3 Nm/rad, or 0.80 ± 0.08 in a normalized vector error score. Comparing the average stiffness among different co-contraction levels, the stiffness coefficients in the DP anatomical axis showed more dependence to the muscle contraction than the IE axis: 4.6 Nm/rad per % MVC and 1.1 Nm/rad per % MVC, respectively.

To accurately estimate the ankle impedance parameters as a function of the EMG signals, different regression models and EMG parameter features were evaluated. The best model used 24 EMG features: the mean, standard deviation, mean absolute value, number of zero crossings, number of slope sign changes, and the cumulative length of each of the 4 raw EMG signals. The best regression model to fit the stiffness and damping in DP was the Least Square method with Regularization, and the best for IE stiffness was the Gaussian Process Regression. The estimation of IE damping did not perform well, possibly because this parameter did not change very much with increased muscle co-contraction.

REFERENCES

[1] C. Castellini *et al.*, "Proceedings of the first workshop on Peripheral Machine Interfaces: going beyond traditional surface electromyography," *Front Neurorobot,* vol. 8, p. 22, 2014.

[2] K. Englehart and B. Hudgins, "A robust, real-time control scheme for multifunction myoelectric control," *IEEE Trans Biomed Eng,* vol. 50, no. 7, pp. 848-54, Jul 2003.

[3] F. Zhang and H. Huang, "Source selection for real-time user intent recognition toward volitional control of artificial legs," *IEEE J Biomed Health Inform,* vol. 17, no. 5, pp. 907-14, Sep 2013.

[4] A. Ziai and C. Menon, "Comparison of regression models for estimation of isometric wrist joint torques using surface electromyography," *J Neuroeng Rehabil,* vol. 8, p. 56, Sep 26 2011.

[5] J. Wang, O. A. Kannape, and H. Herr, "Proportional EMG Control of Ankle Plantar Flexion in a Powered Transtibial Prosthesis," presented at the IEEE International Conference on Rehabilitation Robotics, Seattle, Washington USA, 2013.

[6] S. Farmer, S. Silver-Thorn, P. Voglewede, and S. A. Beardsley, "Within-socket myoelectric prediction of continuous ankle kinematics for control of a powered transtibial prosthesis," *J Neural Eng,* vol. 11, no. 5, p. 056027, Oct 2014.

[7] H. Lee, H. I. Krebs, and N. Hogan, "Multivariable dynamic ankle mechanical impedance with active muscles," *IEEE Trans Neural Syst Rehabil Eng,* vol. 22, no. 5, pp. 971-81, Sep 2014.

[8] L. Knop, G. A. Ribeiro, E. M. Ficanha, and M. Rastgaar, "Estimating the relationship between multivariable standing ankle impedance and lower extremity muscle activation," in *IEEE International Conference on Biomedical Robotics and Biomechatronics*, Enschede, Netherland, 2018.

[9] L. Knop, G. A. Ribeiro, and M. Rastgaar, "Correlation between Ankle Impedance and EMG Signals," presented at the International Conference on Neurorehabilitation, Pisa, Italy, 2018.

[10] E. M. Ficanha, G. A. Ribeiro, L. Knop, and M. Rastgaar, "Time-Varying Impedance of the Human Ankle in the Sagittal and Frontal Planes during Straight Walk and Turning Steps," presented at the International Conference on Rehabilitation Robotics, London, 2017.

[11] E. M. Ficanha, G. A. Ribeiro, and M. Rastgaar, "Design And Evaluation Of A 2-Dof Instrumented Platform For Estimation Of The Ankle Mechanical Impedance In The Sagittal And Frontal Planes," *IEEE/ASME Transactions on Mechatronics,* vol. 21, no. 5, pp. 2531-2542, 2016.

[12] M. Rastgaar, H. Lee, E. M. Ficanha, P. Ho, H. I. Krebs, and N. Hogan, "Multi-Directional Dynamic Mechanical Impedance of the Human Ankle: a Key to Anthropomorphism in Lower Extremity Assistive Robots," in *Neuro-Robotics: From Brain Machine Interfaces to Rehabilitation Robotics*, P. Artemiadis, Ed. New York: Springer, 2014, pp. 85-103.

[13] H. Lee and N. Hogan, "Time-Varying Ankle Mechanical Impedance During Human Locomotion," *IEEE Trans Neural Syst Rehabil Eng,* vol. 23, no. 5, pp. 755-64, Sep 2015.

[14] E. J. Rouse, L. J. Hargrove, E. J. Perreault, and T. A. Kuiken, "Estimation of human ankle impedance during the stance phase of walking," *IEEE Trans Neural Syst Rehabil Eng,* vol. 22, no. 4, pp. 870-8, Jul 2014.

[15] I. Di Giulio, C. N. Maganaris, V. Baltzopoulos, and I. D. Loram, "The proprioceptive and agonist roles of gastrocnemius, soleus and tibialis anterior muscles in maintaining human upright posture," *J Physiol,* vol. 587, no. Pt 10, pp. 2399-416, May 15 2009.

[16] A. Savitzky and M. J. E. Golay, "Smoothing and differentiation of data by simplified least squares procedures," *Analytical chemistry,* vol. 3, no. 6, pp. 1627-1639, 1964.

[17] P. Spellucci, "A new technique for inconsistent QP problems in the SQP method," *Mathematical Methods of Operations Research,* vol. 47, no. 3, pp. 355-400, 1998.

[18] T. Baldacchino, W. R. Jacobs, S. R. Anderson, K. Worden, and J. Rowson, "Simultaneous Force Regression and Movement Classification of Fingers via Surface EMG within a Unified Bayesian Framework," *Front Bioeng Biotechnol,* vol. 6, p. 13, 2018.

[19] B. Hudgins, P. Parker, and R. N. Scott, "A New Strategy for Multifunction Myoelectric Control," *IEEE Trans Biomed Eng,* vol. 40, no. 1, p. 82, 1993.

[20] Y. Huang, K. B. Englehart, B. Hudgins, and A. D. C. Chan, "A Gaussian Mixture Model Based Classification Scheme for Myoelectric Control of Powered Upper Limb Prostheses," *IEEE Transactions on Biomedical Engineering,* vol. 52, no. 11, pp. 1801-1811, 2005.

[21] A. Phinyomark, F. Quaine, S. Charbonnier, C. Serviere, F. Tarpin-Bernard, and Y. Laurillau, "EMG feature evaluation for improving myoelectric pattern recognition robustness," *Expert Systems with Applications,* vol. 40, no. 12, pp. 4832-4840, 2013.

[22] C. M. Bishop, *Pattern Recognition and Machine Learning (Information Science and Statistics)*. 2006.

[23] P. L. Weiss, I. W. Hunter, and R. E. Kearney, "Human ankle joint stiffness over the full range of muscle activation level," *Journal of Biomechanics,* vol. 21, no. 7, pp. 539-544, 1988.